

## Synergism of 1D/2D boride/MXene nanosheets heterojunctions for boosted overall water splitting

Xinyu Ding<sup>a#</sup>, Xunyu Wang<sup>a#</sup>, Wenwu Song<sup>a</sup>, Xiaoqing Wei<sup>a</sup>, Jinli Zhu<sup>a\*</sup>, Yanfeng Tang<sup>a,b</sup>, Minmin Wang<sup>a,b\*</sup>

<sup>a</sup> School of Chemistry and Chemical Engineering, Nantong University, Nantong 226019, China

<sup>b</sup> Nantong Key Laboratory of Intelligent and New Energy Materials

\*Corresponding authors' E-mail: [mmwang0528@ntu.edu.cn](mailto:mmwang0528@ntu.edu.cn); [jinlizhu@ntu.edu.cn](mailto:jinlizhu@ntu.edu.cn)

# These authors contributed equally to this work.

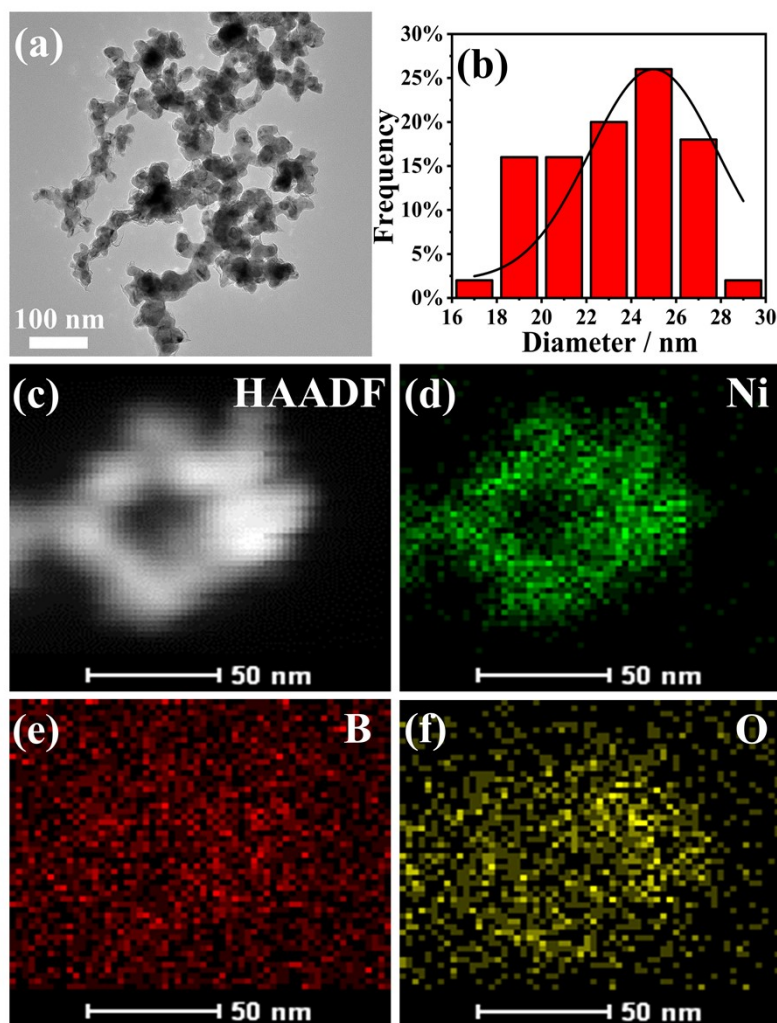


**Figure S1.** (a) TEM images of  $\text{Ni}_x\text{B}$ . (b)  $\text{Ni}_x\text{B}$  nanoparticles size distribution. (c) HAADF image, and (d-f) its corresponding elemental mapping images of  $\text{Ni}_x\text{B}$ .

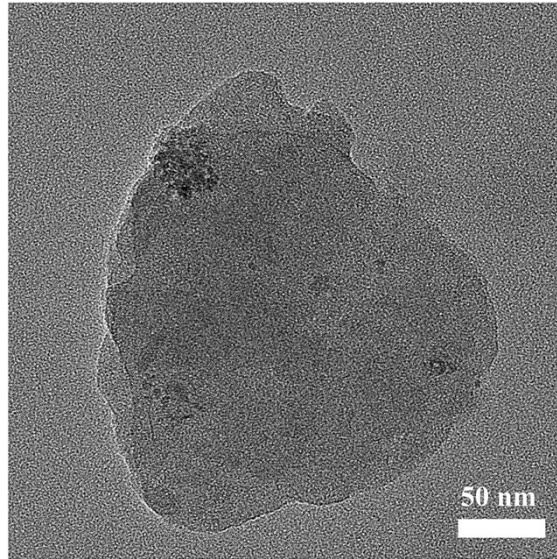


Figure S2. TEM image of N<sub>10</sub>TC nanosheets.

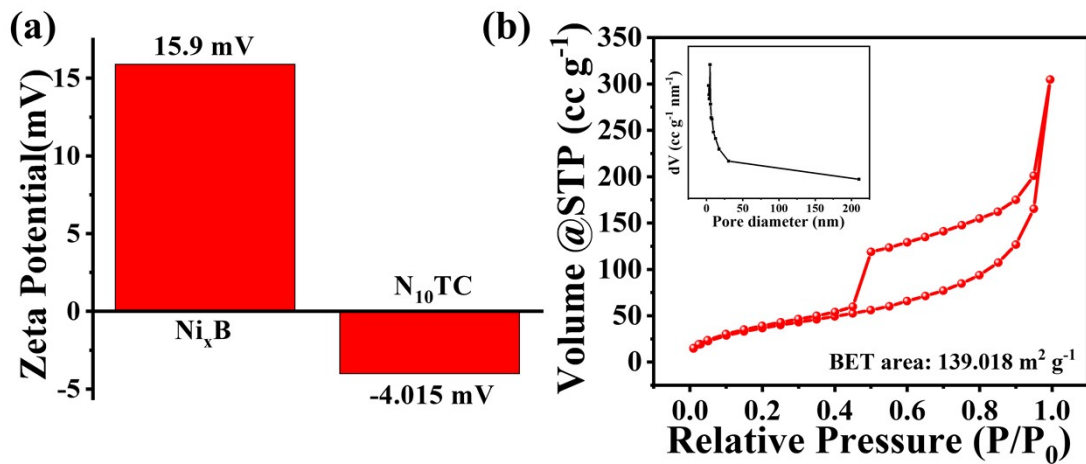


Figure S3. (a) Zeta potentials of Ni<sub>x</sub>B and N<sub>10</sub>TC dispersed in water. (b) N<sub>2</sub>-sorption isotherm of Ni<sub>x</sub>B/N<sub>10</sub>TC, the inset shows the pore size distribution.

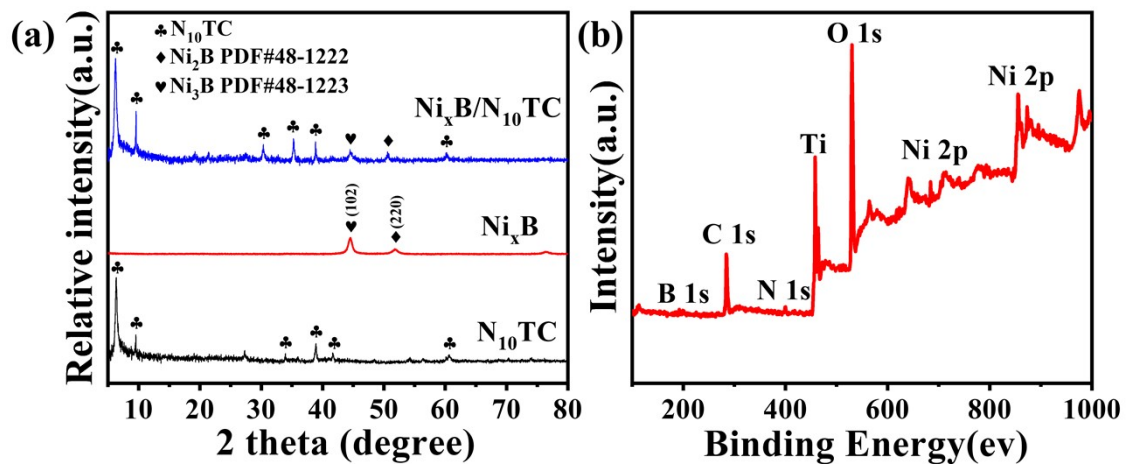
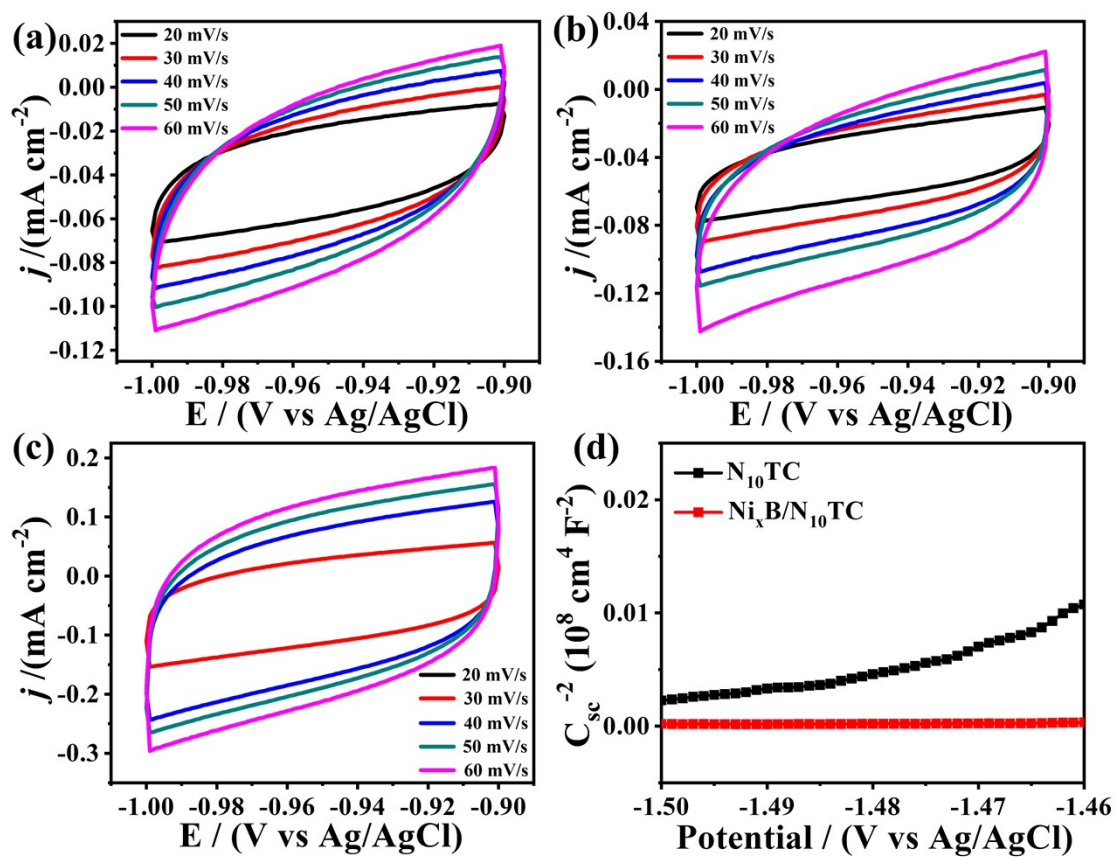
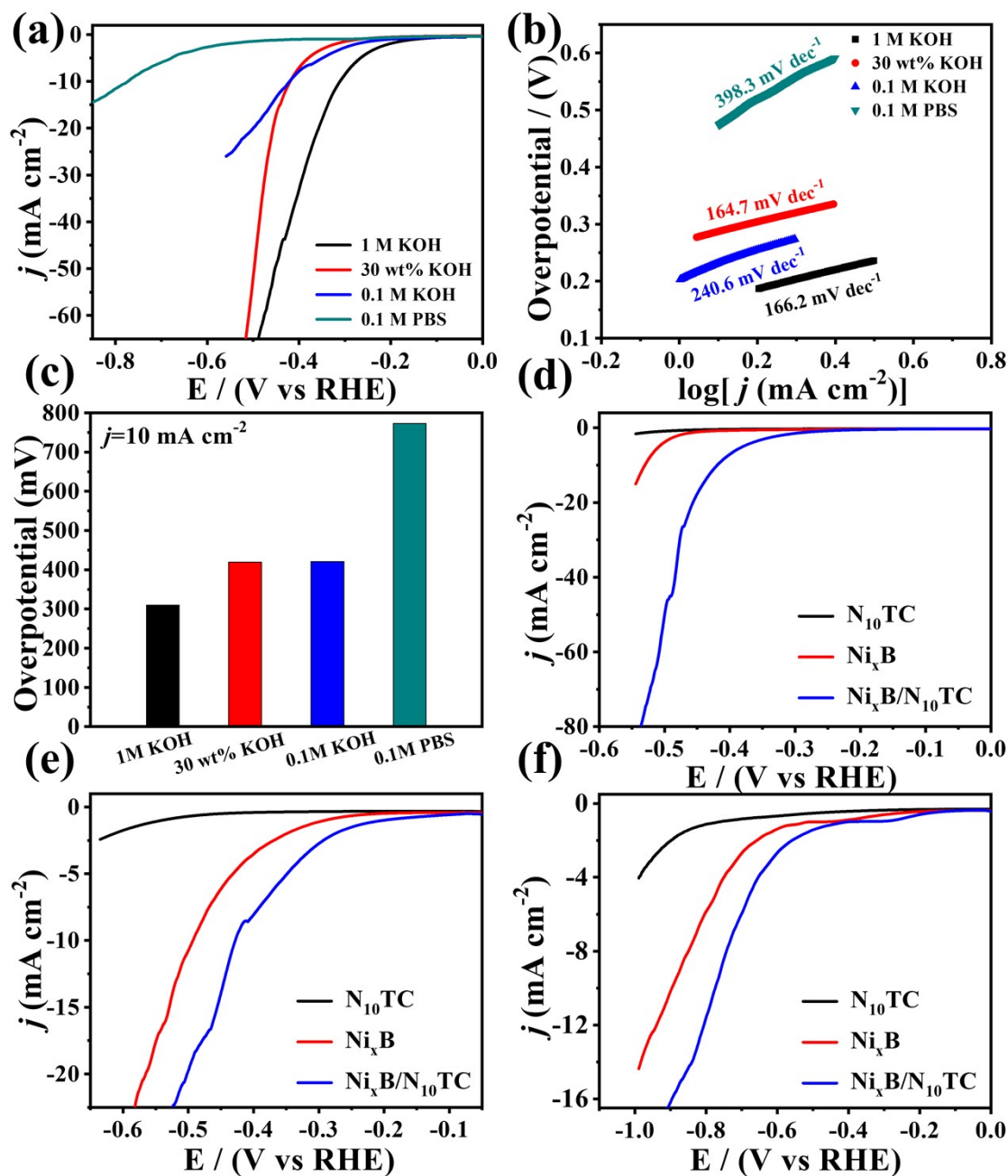


Figure S4. (a) PXRD patterns of Ni<sub>x</sub>B/N<sub>10</sub>TC, Ni<sub>x</sub>B, and N<sub>10</sub>TC. (b) XPS survey spectra of Ni<sub>x</sub>B/N<sub>10</sub>TC.



**Figure S5.** Cyclic voltammograms at different scan rate in the region of -0.9 ~ -1 V vs. Ag/AgCl for (a)  $N_{10}TC$ , (b)  $Ni_xB$  and (c)  $Ni_xB/N_{10}TC$ . (d) Mott-Schottky plots for  $N_{10}TC$  and  $Ni_xB/N_{10}TC$  at 1 kHz frequency in 1 M KOH (pH = 14) at room temperature.



**Figure S6.** (a) HER polarization curves of  $\text{Ni}_x\text{B}/\text{N}_{10}\text{TC}$  in different electrolytes; (b) Tafel slopes and corresponding exchange current density ( $j_0$ ); (c) Overpotentials at 10  $\text{mA cm}^{-2}$  for  $\text{Ni}_x\text{B}/\text{N}_{10}\text{TC}$  electrode in different electrolytes. (d-f) HER polarization curves ( $1 \text{ mV s}^{-1}$ ) of different electrodes in different electrolytes, (d) 30 wt% KOH; (e) 0.1 M KOH; (f) 0.1 M PBS (pH=7) solution.

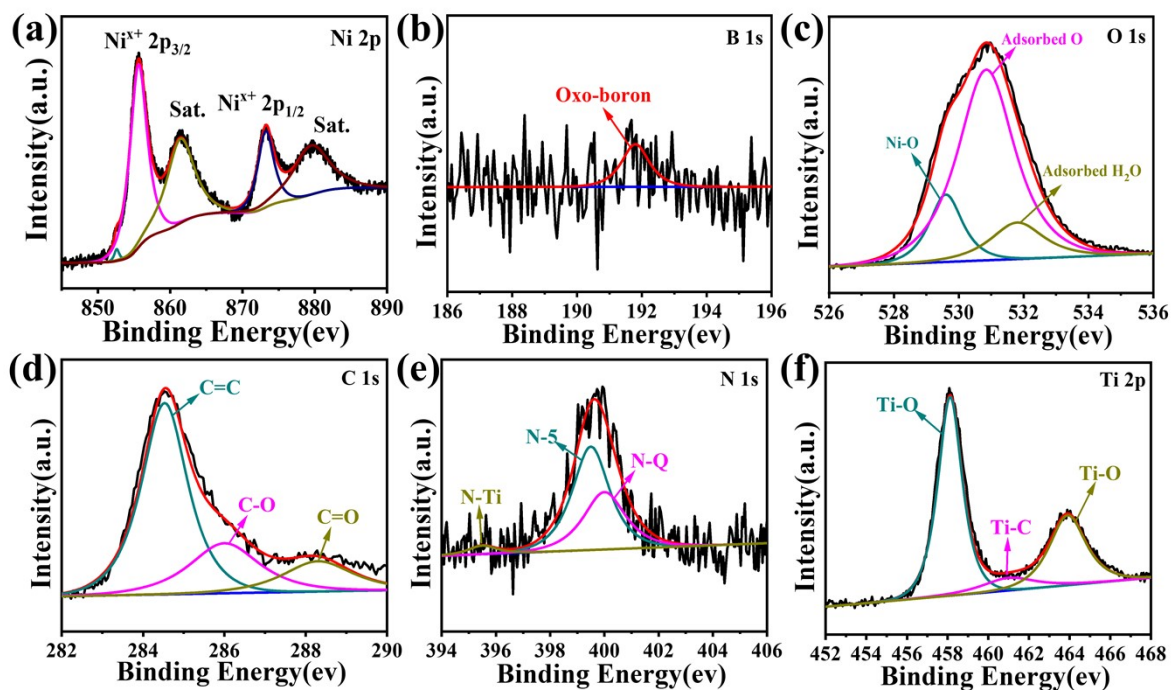


Figure S7. XPS spectra of  $\text{Ni}_x\text{B}/\text{N}_{10}\text{TC}$  heterojunction after 1000 cycles test.

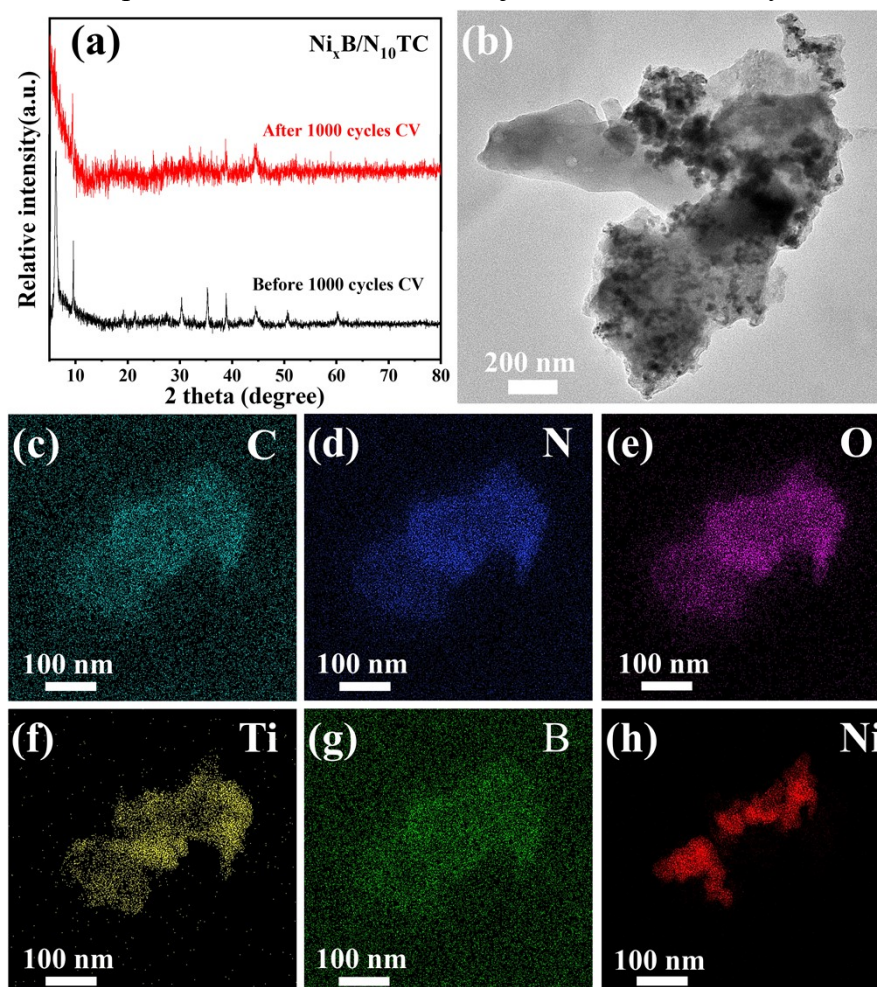
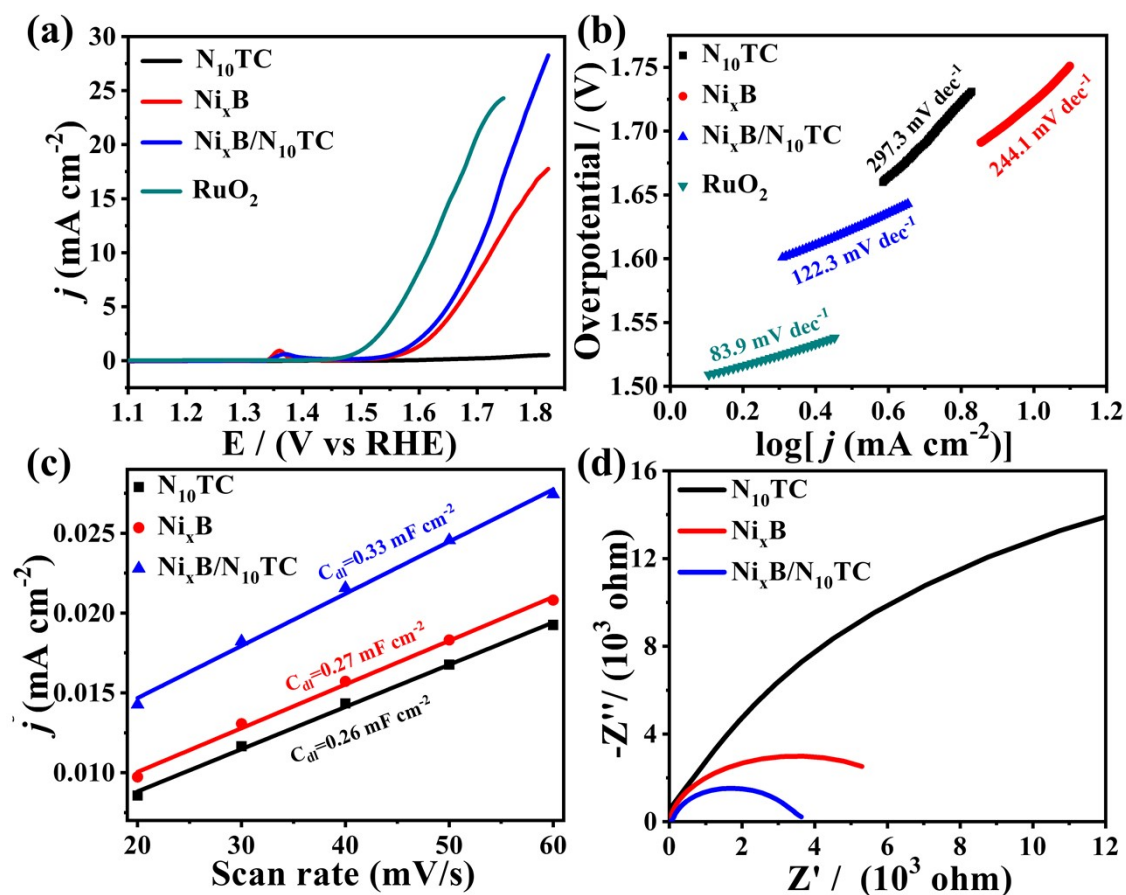
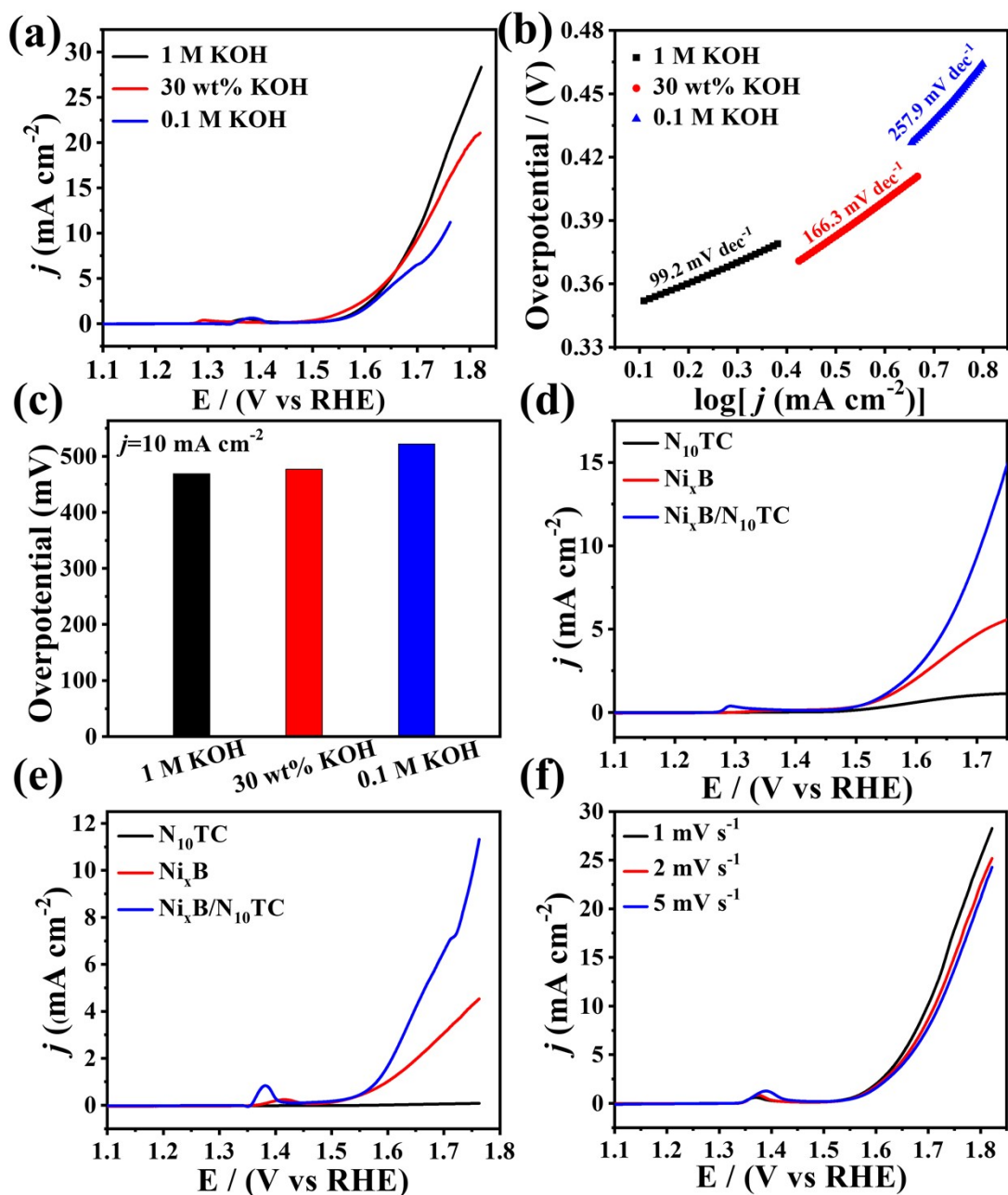


Figure S8. (a) XRD, (b)TEM and (c-h) its corresponding elemental mapping for the sample of  $\text{Ni}_x\text{B}/\text{N}_{10}\text{TC}$  heterojunction after HER stability test.



**Figure S9.** (a) Polarization curves with 80% iR-compensation and (b) Tafel plots of  $N_{10}TC$ ,  $Ni_xB$ ,  $Ni_xB/N_{10}TC$ , and commercial  $RuO_2$  for OER in 1.0 M KOH electrolyte. (c)  $C_{dl}$  values estimated in 1.0 M KOH electrolyte. (d) Electrochemical impedance spectroscopy of  $N_{10}TC$ ,  $Ni_xB$ ,  $Ni_xB/N_{10}TC$ .



**Figure S10.** (a) OER polarization curves of  $\text{Ni}_x\text{B}/\text{N}_{10}\text{TC}$  in different electrolytes; (b) Tafel slopes and corresponding exchange current density ( $j_0$ ); (c) Overpotentials at 10  $\text{mA cm}^{-2}$  for  $\text{Ni}_x\text{B}/\text{N}_{10}\text{TC}$  electrode in different electrolytes. (d-e) OER polarization curves ( $1 \text{ mV s}^{-1}$ ) of different electrodes in different electrolytes, (d) 30 wt% KOH; (e) 0.1 M KOH. (f) OER polarization curves of  $\text{Ni}_x\text{B}/\text{N}_{10}\text{TC}$  heterojunction under various sweep speeds.

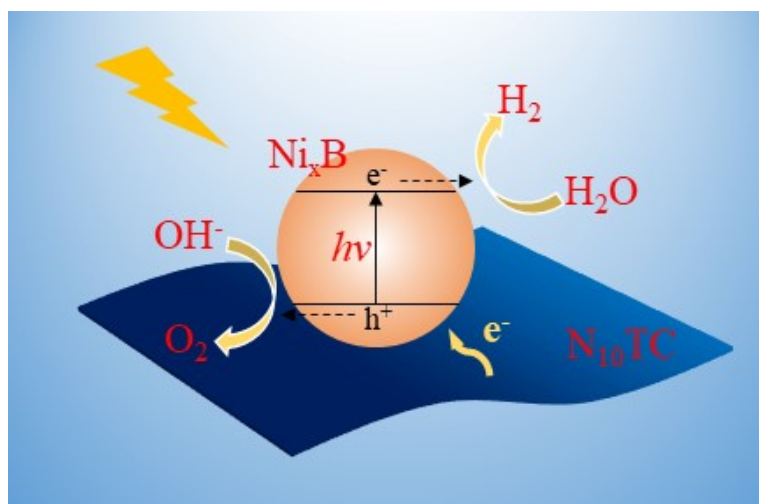


Figure S11 The potential mechanism of the catalysis process.



**Table S1** Comparison of catalytic performance with the most recently reported water-splitting catalysts.

Catalyst	Substrate used	Electrolyte	Loading amount (mg cm <sup>-2</sup> )	$\eta_{10}$ (mV)		A/g	Ref.
				HER	OER		
<b>Ni<sub>x</sub>B/N<sub>10</sub>TC</b>	<b>GC</b>	<b>1 M KOH</b>	<b>0.11</b>	<b>310</b>	<b>468</b>	<b>90.91</b>	<b><i>This work</i></b>
Ni <sub>2</sub> B-gC <sub>3</sub> N <sub>4</sub>	GC	1 M KOH	—	707	—	—	<i>ACS Sustainable Chem. Eng.</i> <b>2018</b> , <i>6</i> , 16198
Ni <sub>x</sub> B-300	GC	1 M KOH	0.21	—	380	47.62	<i>Adv. Energy Mater.</i> <b>2017</b> , <i>7</i> , 1700381
Co <sub>2</sub> B-CoSe <sub>2</sub>	GC	1 M KOH	0.40	300	320	25	<i>ACS Appl. Mater. Interfaces</i> <b>2017</b> , <i>9</i> , 39312
Etched Mo-Al-B	Unsupport ed	0.5 M H <sub>2</sub> SO <sub>4</sub>	—	361	—	—	<i>Chem. Mater.</i> <b>2017</b> , <i>29</i> , 8953
MoS <sub>2</sub> /Ti <sub>3</sub> C <sub>2</sub>	GC	0.5 M H <sub>2</sub> SO <sub>4</sub>	0.35	280	—	28.57	<i>Int. J. Hydrogen Energy</i> <b>2019</b> , <i>44</i> , 965-976
NiCoS/Ti <sub>3</sub> C <sub>2</sub> T <sub>x</sub>	GC	1 M KOH	0.21	—	365	47.62	<i>ACS Appl Mater Interfaces</i> <b>2018</b> , <i>10</i> , 22311-22319